Supporting Information

Preparation and Properties of an Mn^{IV}–Hydroxide Complex: Proton and Electron Management at a Mononuclear Mn Site and its Relationship to the Oxygen Evolving Complex within Photosystem II

Taketo Taguchi,† Kari L. Stone,|| Rupal Gupta,‡ Benedikt Kaiser-Lassalle,¶ Junko Yano,¶* Michael P. Hendrich,‡* A.S. Borovik†*

Contributed from the †Department of Chemistry, University of California-Irvine, 1102 Natural Sciences II, Irvine, CA 92697; ||Department of Chemistry, Benedictine College, Lisle, IL; ‡Department of Chemistry, Carnegie Mellon University, Pittsburgh, PA 15213; ¶Physical Biosciences Division, Lawrence Berkeley National Laboratory, Berkeley, CA 94720.

E-mail: aborovik@uci.edu; hendrich@andrew.cmu.edu; jyano@lbl.gov

Experimental Section.

General Methods.

All reagents were purchased from commercial sources and used as received unless otherwise noted. Solvents were sparged with argon and dried over columns containing Q-5 and molecular sieves. DMF was stored over activated 4 Å molecular sieves for two days in a Vacuum Atmospheres, Co. drybox under an Ar atmosphere, then decanted onto a second portion of 4 Å molecular sieves for two days before use. The syntheses of metal complexes were conducted in an Ar atmosphere. The preparation of $K_2[Mn^{II}H_3buea(OH)]$, $K_2[Mn^{III}H_3buea(O)]$, $K[Mn^{III}H_3buea(OH)]$, ferrocenium tetrafluoroborate ($[FeCp_2]BF_4$), and triethylammonium tetrafluoroborate ($[HNEt_3]BF_4$) followed the literature procedure.[1]

Preparation of $[Mn^{IV}H_3buea(OH)]$ from $[Mn^{III}H_3buea(OH)]^-$.

UV-Vis Absorbance Measurements. A quartz cuvette containing DMF (1.5 mL) and THF (1.5 mL) under an argon atmosphere was cooled to -80 °C within the spectrophotometer and stirred for 15 min. A solution of $K[Mn^{III}H_3buea(OH)]$ (0.50 μmol, 20 μL of a 25 mM solution in DMF) was added via injection with a gas tight syringe, the mixture was stirred for 1 min, and then treated with 1 equiv of $[FeCp_2]BF_4$ (0.5 μmol, 10 μL of a 50 mM solution in DMF) to produce $[Mn^{IV}H_3buea(OH)]$. The conversion was monitored with optical spectroscopy. A similar procedure was used to generate $[Mn^{IV}H_3buea(OH)]$ from $K_2[Mn^{II}H_3buea(OH)]$ using 2 equiv of $[FeCp_2]BF_4$ (1.0 μmol, 20 μL).

Electron Paramagnetic Resonance Measurements.

A solution of $K_2[Mn^{II}H_3buea(OH)]$ (5.0 μmol, 50 μL of a 100 mM solution in DMF) containing 2 equiv of 18-crown-6 (2.6 mg, 10 μmol) was combined with THF (110 μL) and DMF (20 μL) in an EPR tube, and cooled to -78 °C in an acetone/dry ice bath. After 15 min, the solution was treated with 2 equiv of $[FeCp_2]BF_4$ (10.0 μmol, 40 μL of 250 mM solution in DMF) via injection with a gas tight syringe. The solution was allowed to sit for another 15 min and frozen in liquid N_2. A similar procedure was used to generate

$[Mn^{III}H_3buea(OH)]^-$ using 1 equiv of $[FeCp_2]BF_4$ (5.0 µmol, 40 µL of 250 mM solution in DMF).

Preparation of $[Mn^{IV}H_3buea(OH)]$ from $[Mn^{V}H_3buea(O)]$.

UV-Vis Absorbance Measurements. A quartz cuvette containing DMF (1.5 mL) and THF (1.5 mL) under an argon atmosphere was cooled to -80˚C within the spectrophotometer and stirred for 15 min. A solution of $K_2[Mn^{III}H_3buea(O)]$ (0.50 µmol, 20 µL of a 25 mM solution in DMF) was added via injection with a gas tight syringe, the mixture was stirred for 1 min, and then treated with 2 equiv of $[FeCp_2]BF_4$ (1.0 µmol, 20 µL of a 50 mM solution in DMF) to produce $[Mn^{V}H_3buea(O)]$. The latter solution was then treated with 2,4,6-Tri-*tert*-butylphenol (0.5 µmol, 10 µL of a 50 mM solution in DMF).

Electron Paramagnetic Resonance Measurements.

A solution of $K_2[Mn^{III}H_3buea(O)]$ (4.0 µmol, 40 µL of a 100 mM solution in DMF) containing 2 equiv of 18-crown-6 (2.1 mg, 8.0 µmol) was combined with THF (100 µL) in an EPR tube and cooled to -78˚C in an acetone/dry ice bath. After 15 min, the solution was treated with 2 equiv of $[FeCp_2]BF_4$ (8.0 µmol, 40 µL of 200 mM solution in DMF) via injection with a gas tight syringe to produce $[Mn^{V}H_3buea(O)]$. The latter solution was then treated with 2,4,6-tri-*tert*-butylphenol (TBP) (4.0 µmol, 20 µL of a 200 mM solution in DMF). The solution was allowed to sit for another 15 min and frozen in liquid N_2.

Preparation of $[Mn^{IV}H_3buea(OH)]$ from $[Mn^{IV}H_3buea(O)]^-$.

UV-Vis Absorbance Measurements. A quartz cuvette containing DMF (1.5 mL) and THF (1.5 mL) under an argon atmosphere was cooled to -80˚C within the spectrophotometer and stirred for 15 min. A solution of $K_2[Mn^{III}H_3buea(O)]$ (0.50 µmol, 20 µL of a 25 mM solution in DMF) was added via injection with a gas tight syringe, the mixture was stirred for 1 min, and then treated with 1 equiv of $[FeCp_2]BF_4$ (0.50 µmol, 10 µL of a 50 mM solution in DMF) to produce $[Mn^{IV}H_3buea(O)]^-$. To the latter was added 1 equiv of $[HNEt_3]BF_4$ (0.50 µmol, 10 µL of a 50 mM solution in DMF) to produce

[$Mn^{IV}H_3buea(OH)$]. The conversion was monitored with optical spectroscopy.

Electron Paramagnetic Resonance Measurements.

A solution of $K_2[Mn^{III}H_3buea(O)]$ (6.0 µmol, 60 µL of a 100 mM solution in DMF) containing 2 equiv of 18-crown-6 (3.2 mg, 1.2 µmol) was combined with THF (150 µL) in an EPR tube and cooled to -78˚C in an acetone/dry ice bath. After 15 min, the solution was treated with 1 equiv of $[FeCp_2]BF_4$ (6.0 µmol, 30 µL of 200 mM solution in DMF) via injection with a gas tight syringe to produce $[Mn^{IV}H_3buea(O)]^-$. The latter solution was then treated with 1 equiv of $[HNEt_3]BF_4$ (6.0 µmol, 60 µL of a 100 mM solution in DMF). The solution was allowed to sit for another 15 min and frozen in liquid N_2.

X-ray Absorption Spectroscopic Measurements

A solution of $K_2[Mn^{II}H_3buea(OH)]$ (25 µmol, 250 µL of a 100 mM solution in DMF) containing 2 equiv of 18-crown-6 (13 mg, 50 µmol) was combined with THF (500 µL) and $[FeCp_2]BF_4$ solution (50 µmol, 125 µL of a 200 mM solution in DMF) at -80˚C under argon in a drybox cold-well. After mixing, a portion of the solution was transferred to a pre-cooled XAS sample holder and frozen in liquid N_2.

Reaction of $[Mn^{III}H_3buea(OH)]^-$ and $[Mn^{V}H_3buea(O)]$. A quartz cuvette containing DMF (1.5 mL) and THF (1.5 mL) under an argon atmosphere was cooled to -80˚C within the spectrophotometer and stirred for 15 min. A solution of $K_2[Mn^{III}H_3buea(O)]$ (0.50 µmol, 20 µL of a 25 mM solution in DMF) was added via injection with a gas tight syringe, the mixture was stirred for 1 min, and then treated with 2 equiv of $[Cp_2Fe]BF_4$ (1.0 µmol, 20 µL of a 50 mM solution in DMF) to produce $[Mn^{V}H_3buea(O)]$. The latter solution was then treated with $K[Mn^{III}H_3buea(OH)]$ (0.50 µmol, 20 µL of a 25 mM solution in DMF). Electronic absorbance spectra were collected on the resultant mixture. For comparison, the reference spectra of equal molar solutions of pure $[Mn^{IV}H_3buea(OH)]$ and $[Mn^{IV}H_3buea(O)]^-$ in DMF/THF (1:1) at -80˚C were collected independently and their spectra were used to produce the reference spectrum.

Reaction of $[Mn^{II}H_3buea(OH)]^{2-}$ and $[Mn^{IV}H_3buea(O)]^-$. In a typical experiment, crystals of $K_2[Mn^{III}H_3buea(O)]$ (25 mg, 0.033 mmol) were dissolved in 2.5 mL of DMSO and a 0.5 mL aliquot of the solution was removed for UV-vis spectroscopy. Solid $[Cp_2Fe]BF_4$ (7.4 mg, 0.027 mmol) was added to the stirring solution and the purple solution immediately turned to a dark green color with identical spectroscopic characteristics as $[Mn^{IV}H_3buea(O)]^-$.**Error! Bookmark not defined.**[c] A 1.0 mL aliquot of this solution was added to a 1.0 mL stirring solution of $K_2[Mn^{II}H_3buea(OH)]$ (11 mg, 0.014 mmol) in DMSO. UV-vis spectra were collected on the resultant mixture.

Physical Methods. Electronic absorbance spectra were recorded with an 8453 Agilent UV-vis spectrometer equipped with an Unisoku Unispeks cryostat. Cyclic voltammetric experiments were conducted using a BAS CV 50W (Bioanalytical Systems Inc., West Lafayette, IN) voltammetric analyzer. A glassy carbon electrode was used as the working electrode to measure the cyclic voltammograms at scan velocities 0.01 $V{\cdot}s^{-1}$. A ferrocenium/ferrocene couple ($[FeCp_2]^{+/0}$) was used as an internal reference. IR compensation was achieved before each CV was recorded. Redox potentials are reported versus the ferrocenium/ferrocene couple.

X-band electron paramagnetic resonance (EPR) spectra were recorded on a Bruker 300 spectrometer equipped with an Oxford ESR-910 liquid helium cryostat and a dual mode microwave cavity. The quantification of signals is relative to a CuEDTA spin standard. The microwave frequency was calibrated with a frequency counter and the magnetic field with a NMR gaussmeter. The modulation frequency and amplitude was 100 kHz and 1.0 mT_{pp}. The EPR simulation software package SpinCount was used to analyze the data.[2] X-ray absorption spectra were collected at the Stanford Synchrotron Radiation Lightsource (SSRL) on beamline 7–3 at an electron energy of 3.0 GeV with an average current of 300 mA. The incoming X-ray was monochromatized by a Si(220) double-crystal monochromator. The intensity of the incident X-ray was monitored by an N_2-filled ion chamber (I_o) in front of the sample. Solution samples were filled in 40 uL plexi glass holder and kept under liquid N_2

until data collection. Data were collected as fluorescence excitation spectra with a Ge 30 element detector (Canberra). The monochromator energy was calibrated by the pre-edge peak top of $KMnO_4$ standard at 6543.30 eV. The standard was placed between two N_2-filled ionization chambers (I_1 and I_2) after the sample. All data were collected at 8K using liquid He flow cryostat (Oxford).

Data reduction of the extended X-ray absorption fine structure (EXAFS) spectra was performed using SixPack (Dr. Samuel Webb, SSRL). Pre-edge and post-edge backgrounds were subtracted from the XAS spectra, and the results were normalized with respect to edge height. Background removal in *k*-space was achieved through a five-domain cubic spline. Curve fitting was performed with Artemis and IFEFFIT software using *ab initio*-calculated phases and amplitudes from the program FEFF 8.2.[3,4] These *ab initio* phases and amplitudes were used in the EXAFS equation:

$$\chi(k) = S_0^2 \sum_j \frac{N_j}{kR_j^2} f_{eff_j}(\pi,k,R_j) e^{-2\sigma_j^2 k^2} e^{-2R_j/\lambda_j(k)} \sin(2kR_j + \phi_{ij}(k)) \qquad (1)$$

The neighboring atoms to the central atom(s) are divided into *j* shells, with all atoms with the same atomic number and distance from the central atom grouped into a single shell. Within each shell, the coordination number N_j denotes the number of neighboring atoms in shell *j* at a distance of R_j from the central atom. The term $f_{eff_j}(\pi,k,R_j)$ is the *ab initio* amplitude function for shell *j*, and the Debye-Waller term $e^{-2\sigma_j^2 k^2}$ accounts for damping due to static and thermal disorder in absorber-backscatterer distances. The mean free path term $e^{-2R_j/\lambda_j(k)}$ reflects losses due to inelastic scattering, where $\lambda_j(k)$ is the electron mean free path. The oscillations in the EXAFS spectrum are reflected in the sinusoidal term, $\sin(2kR_j + \varphi_{ij}(k))$ where $\varphi_{ij}(k)$ is the *ab initio* phase function for shell *j*. S_o^2 is an amplitude reduction factor due to shake-up/shake-off processes at the central atom(s). The EXAFS equation was used to fit the experimental data using *N*, *R*, and the EXAFS Debye-Waller factor (σ^2) as variable parameters. E_o was defined as 6545.0 eV and the S_o^2 value was fixed to 0.85 for the energy (eV) to wave vector (*k*, $Å^{-1}$) axis conversion.

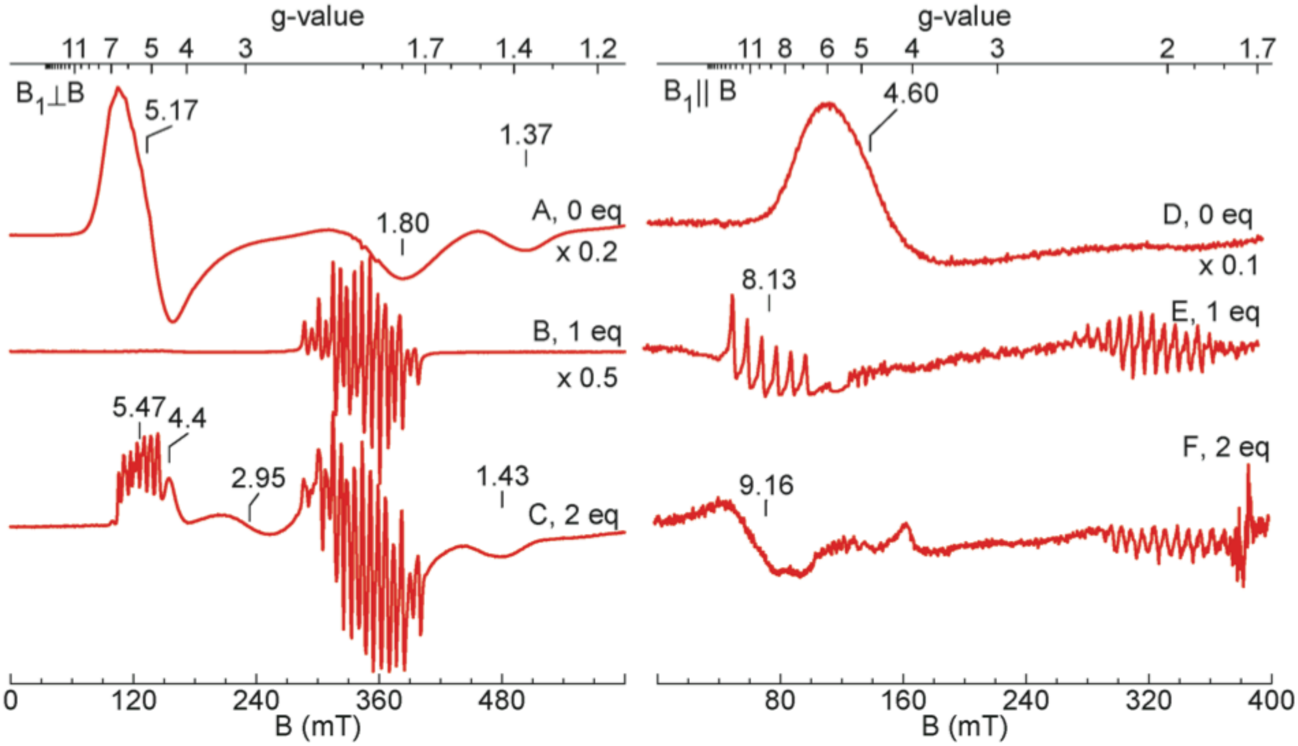

Figure S1. Perpendicular (left side) and parallel (right side) mode EPR spectra of (A, D) 10 mM $[Mn^{II}H_3buea(OH)]^{2-}$; (B, E) + 1 eq $[Cp_2Fe]BF_4$ to form $[Mn^{III}H_3buea(OH)]^{-}$; and (C, F) + 2 eq $[Cp_2Fe]BF_4$ to form $[Mn^{IV}H_3buea(OH)]$. Experimental condition: temperature 10K, power 0.2 mW, frequency 9.6 (perpendicular-mode), 9.3 (parallel-mode) GHz.

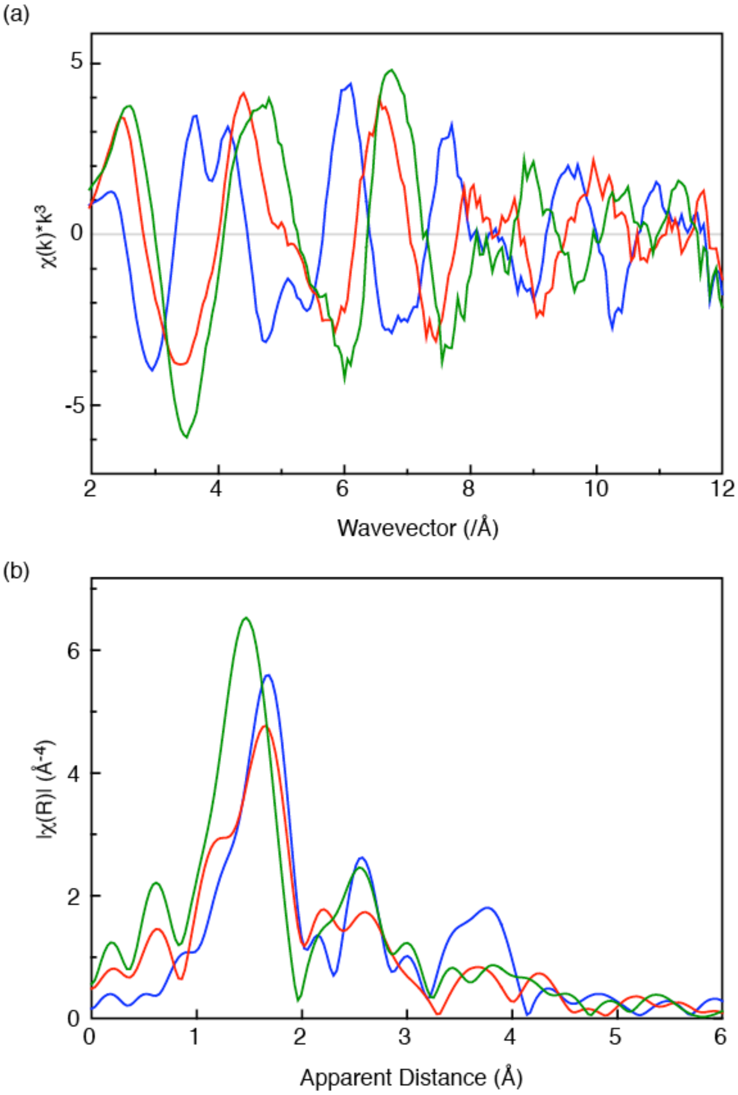

Figure S2. (a) k^3-weighted Mn EXAFS and (b) FT-EXAFS spectra of compounds of $[Mn^{II}H_3buea(OH)]^{2-}$ (blue), $[Mn^{III}H_3buea(OH)]^{-}$ (red), and $[Mn^{IV}H_3buea(OH)]$ (green).

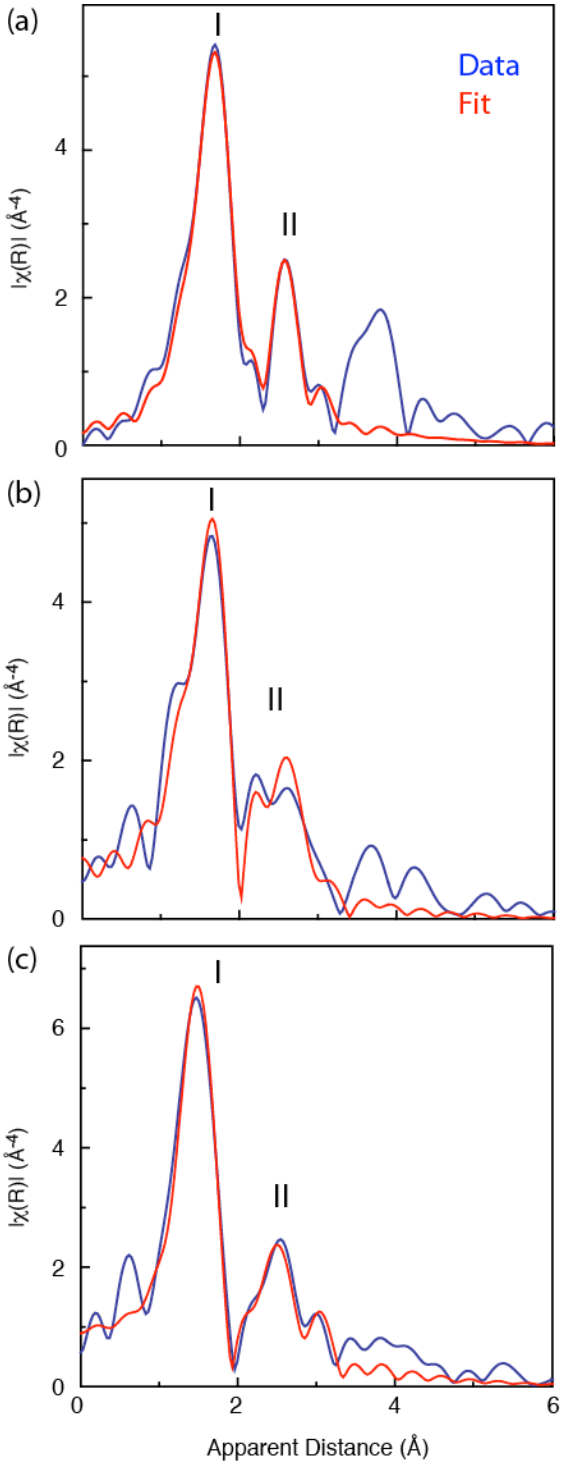

Figure S3. EXAFS curve fitting results of compound of (a) $[Mn^{II}H_3buea(OH)]^{2-}$, (b) $[Mn^{III}H_3buea(OH)]^{-}$, and (c) $[Mn^{IV}H_3buea(OH)]$. The R range of 0.98 to 3.3 Å were used for the fitting. The experimental data are in blue and calculated fits are in red.

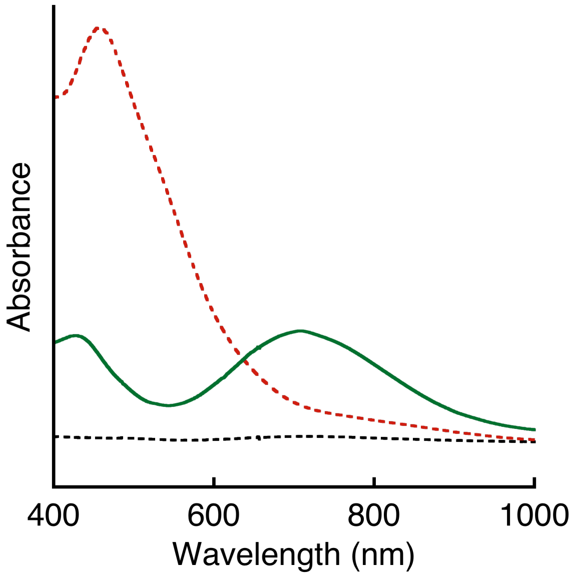

Figure S4. Electronic absorbance spectra of [Mn^{II}H$_3$buea(OH)]$^{2-}$ (black), [Mn^{IV}H$_3$buea(OH)] (red), and the product of equimolar amounts of [Mn^{IV}H$_3$buea(OH)] and [Mn^{II}H$_3$buea(OH)]$^{2-}$ collected at −80 °C in 1:1 THF/DMF.

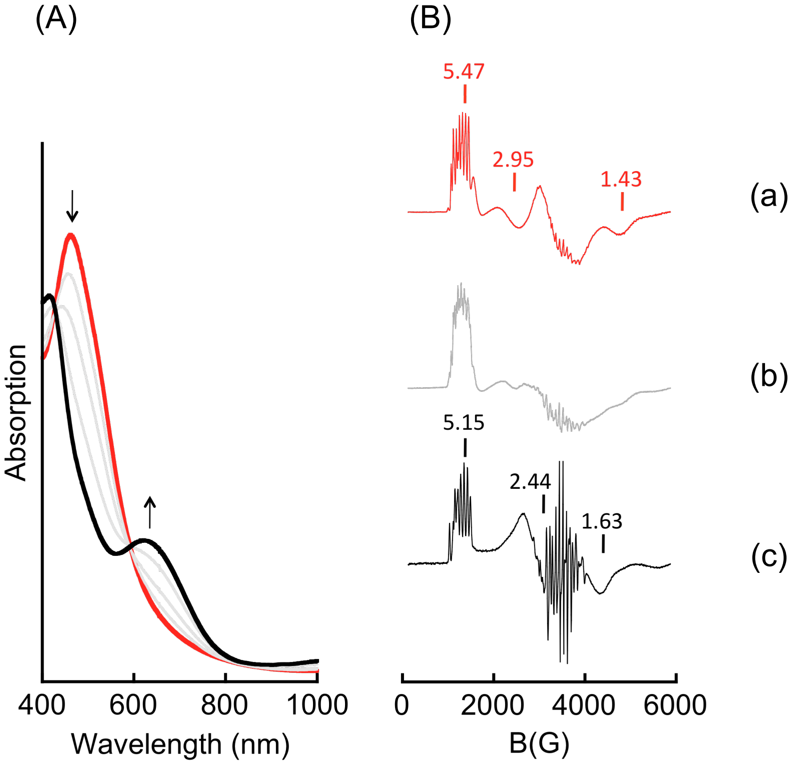

Figure S5. (A) Electronic absorption spectra collected at −80 °C in 1:1 THF/DMF. $[Mn^{IV}H_3buea(OH)]^-$ (red), after the addition of 0.25, 0.5, 0.75, 1.0 (black) equiv of $^tBuO^-$ to $[Mn^{IV}H_3buea(OH)]$. (B) Perpendicular mode EPR spectra of (a) $[Mn^{IV}H_3buea(OH)]$, (b) after the addition of 0.5 equiv of $^tBuO^-$ to $[Mn^{IV}H_3buea(OH)]$, (c) after the addition of 1.0 equiv of $^tBuO^-$ to $[Mn^{IV}H_3buea(OH)]$. Experimental condition: in 1:1 THF/DMF, temperature 5K, frequency 9.6 GHz.

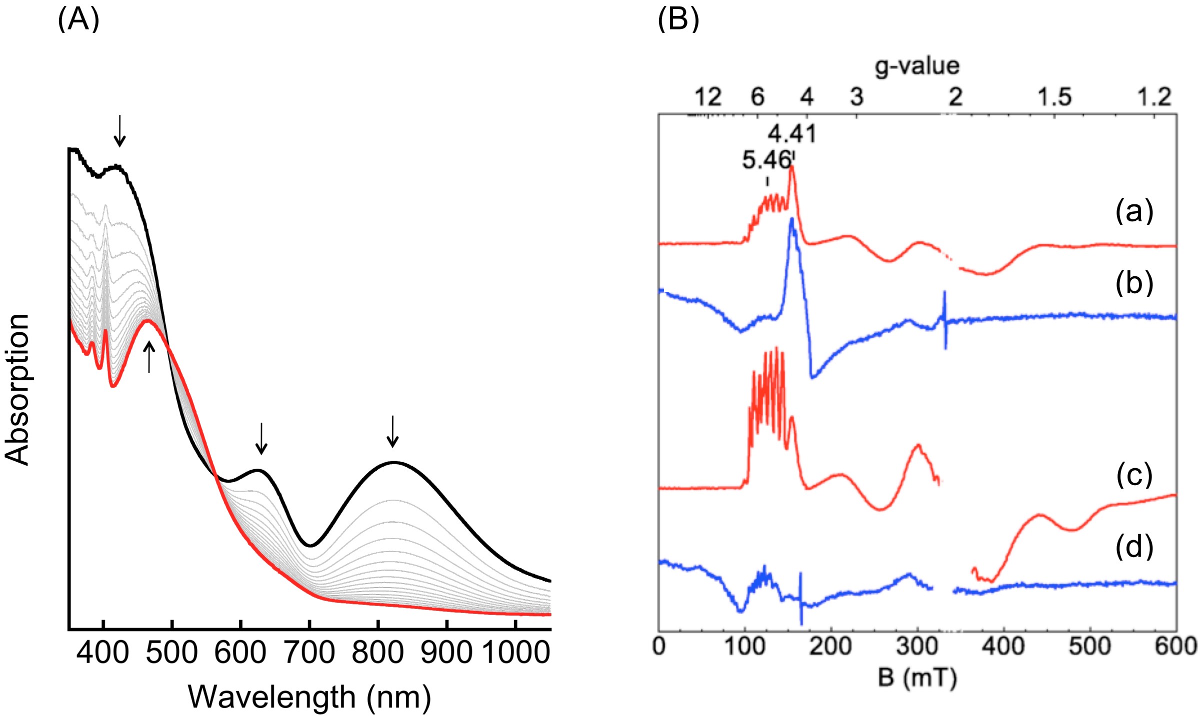

Figure S6. (A) Electronic absorption spectra for the reaction of 1 equiv of TBP with $[\mathrm{Mn^{V}H_3buea(O)}]$ collected at −80 °C in 1:1 THF/DMF. $[\mathrm{Mn^{V}H_3buea(O)}]$ (black) and final spectrum after the addition of TBP (red, $[\mathrm{Mn^{IV}H_3buea(OH)}]$). Spectra depicted in grey line are obtained every 400 seconds after the addition of TBP. (B) EPR spectra of (a) 10 mM $\mathrm{Mn^{V}}$-O in DMF/THF, $B_1 \perp B$, (b) 10 mM $[\mathrm{Mn^{V}H_3buea(O)}]$ in DMF/THF, $B_1 || B$, (c) 10 mM $[\mathrm{Mn^{V}H_3buea(O)}]$ in DMF/THF + 1 eq. 2, 4, 6-tri-*tert*-butylphenol, $B_1 \perp B$, (d) 10 mM $[\mathrm{Mn^{V}H_3buea(O)}]$ in DMF/THF + 1 eq. 2, 4, 6-tri-*tert*-butylphenol, $B_1 || B$. Experimental condition: temperature 10K, power 0.2 mW, frequency 9.63 (A, C), 9.30 (B, D) GHz. A large radical signal due to the oxidation of 2, 4, 6-tri-*tert*-butylphenol was observed at g = 2 and masked in the figure for clarity.

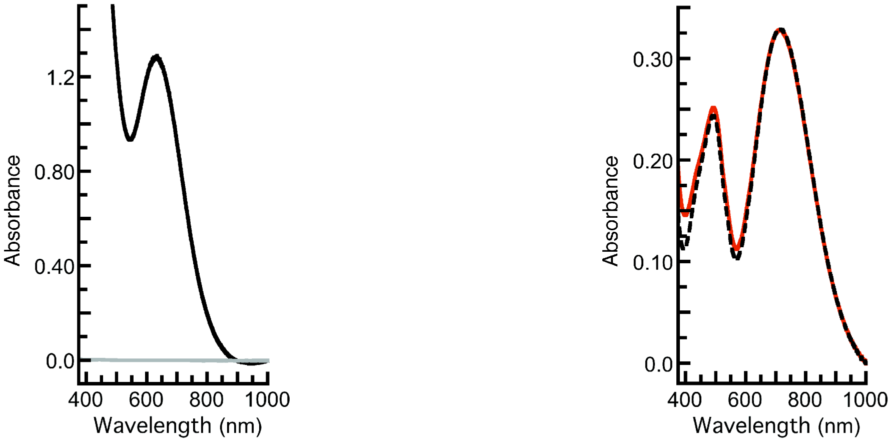

$$[\mathrm{Mn^{IV}H_3buea(O)}]^- + [\mathrm{Mn^{II}H_3buea(OH)}]^{2-} \xrightarrow[\mathrm{rt}]{\mathrm{DMSO}} [\mathrm{Mn^{III}H_3buea(OH)}]^- + [\mathrm{Mn^{III}H_3buea(O)}]^{2-}$$

Figure S7. Visible absorbance spectra, recorded in DMSO at room temperature, for reactants $[\mathrm{Mn^{II}H_3buea(OH)}]^{2-}$ (—) and $[\mathrm{Mn^{IV}H_3buea(O)}]^-$ (—), product mixture (—), and a model spectrum showing a 45(5):55(5) mixture of $[\mathrm{Mn^{III}H_3buea(O)}]^{2-}$ and $[\mathrm{Mn^{III}H_3buea(OH)}]^-$ (---). The absorbance band from ferrocence (produced in generating the $\mathrm{Mn^{IV}{=}O}$ complex, Scheme 1) has been subtracted from the spectra.

References

1. R. Gupta, C. E. MacBeth, J. V. G. Young and A. S. Borovik, *J. Am. Chem. Soc.*, 2002, **124**, 1136; C. E. MacBeth, R. Gupta, K. R. Mitchell-Koch, J. V. G. Young, G. H. Lushington, W. H. Thompson, M. P. Hendrich and A. S. Borovik, *J. Am. Chem. Soc.*, 2004, **126**, 2556; T. Taguchi, R. Gupta, B. Lassalle-Kaiser, D. W. Boyce, V. Yachandra, W. B. Tolman, J. Yano, M. P. Hendrich and A. S. Borovik, *J. Am. Chem. Soc.,* 2012, **134**, 1996; N. G. Connelly and W. E. Geiger, *Chem. Rev.* **1996**, *96*, 877-910; K. Abdur-Rashid, T. P. Fong, B. Greaves, D. G. Gusev, J. G. Hinman, S. E. Landau, A. J. Lough and R. H. Morris, *J. Am. Chem. Soc*. 2000, **122**, 9155.

2. A. P. Golombek and M. P. Hendrich, *J. Magn. Reson.* 2003, **165**, 33.

3.M. Newville, *J. Synchrotron Rad.* 2001, **8**, 322.

4.Rehr, J. J.; Albers, R. C. *Rev. Mod. Phys.* **2000**, *72*, 621.